Solar Wind Mass-Loading Due to Dust

A. Rasca[1,2], M. Horányi[1,3]

[1]*Laboratory for Atmospheric and Space Physics, Boulder, CO, USA*
[2]*Department of Applied Mathematics,* [3]*Department of Physics, University of Colorado at Boulder*

I. Abstract

Collisionless mass-loading by interplanetary dust particles is expected to cause a significant disruption in the flow of the solar wind. Dust particles near the Sun can become a source of ions and neutrals due to evaporation and sputtering. This mass-loading effect can lead to the formation of collisionless shocks, as it was first discussed in the case of solar wind interaction with comets. This effect can also be compared with a de Laval nozzle, which behaves differently between subsonic and supersonic flows. We investigate the effects of mass-loading resulting from sun-grazing comets or collisions in the vicinity of the Sun, where the solar wind transitions from subsonic to supersonic speeds. We implement a hydrodynamic numerical model to generate a steady wind extending out to the inner heliosphere. Dust is introduced through a set of mass-loading source terms, and the model is evolved using a shock-capturing scheme. These results are relevant for understanding the acceleration of the solar wind and possible changes in its composition due to dust.

II. Motivation

Solar wind and dust interactions through collisionless mass-loading due to photoionization were first modeled with the pick-up of cometary ions, affecting both the wind acceleration and its composition (Biermann et al., 1967). Detection of such changes via remote space probe instruments indicate the presence of an interplanetary dust source upstream. We aim to predict the effects of mass-loading upstream in the corona using a simple time-dependent hydrodynamic model.

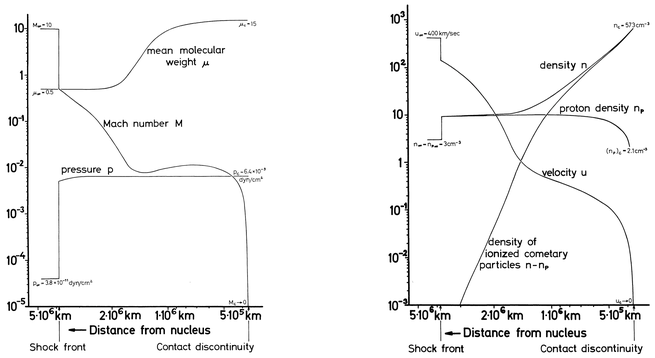

Figure 1: Model results for mass-loading due to a comet (Biermann et al., 1967).

III. Numerical Model

The solar wind is modeled by solving the inviscid spherically symmetric hydrodynamic equations for conservation of mass, momentum, and energy with appropriate source terms added:

$$\frac{\partial \rho}{\partial t} + \frac{\partial}{\partial r}(\rho u) = A$$

$$\frac{\partial}{\partial t}(\rho u) + \frac{\partial}{\partial r}\left(\rho u^2\right) + \frac{\partial p}{\partial r} = B$$

$$\frac{\partial}{\partial t}\left(\frac{1}{2}\rho u^2 + \frac{p}{\gamma - 1}\right) + \frac{\partial}{\partial r}\left[u\left(\frac{1}{2}\rho u^2 + \frac{\gamma}{\gamma - 1}p\right)\right] = C$$

For 1D tests at about 1 AU most source terms can be ignored except those due to mass-loading. Closer to the sun other sources are added, including gravity, spherical expansion, heat conduction, radiative losses, and coronal heating. The equations are solved using Godunov's scheme with Roe's Riemann solver.

IV. Results: Mass-Loading

Mass-loading is first tested in solar wind conditions matching 1 AU. A block distribution of dust is introduced and the solar wind relaxes to a new steady-state.

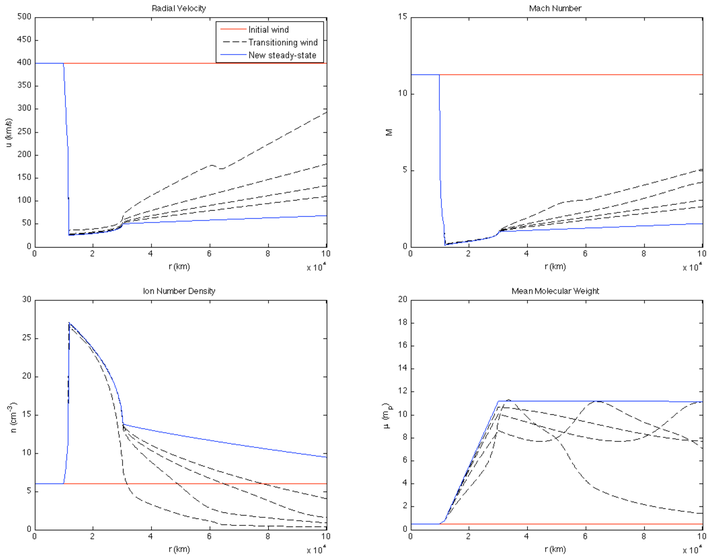

Figure 2: The solar wind relaxing to a new steady-state, matching results from forcing the it through a nozzle using the effective area function (Gombosi et al., 1986).

Nearer the sun, a similar distribution of dust is introduced in three different cases: Before, on, and after the steady-state sonic point in solar radii R.

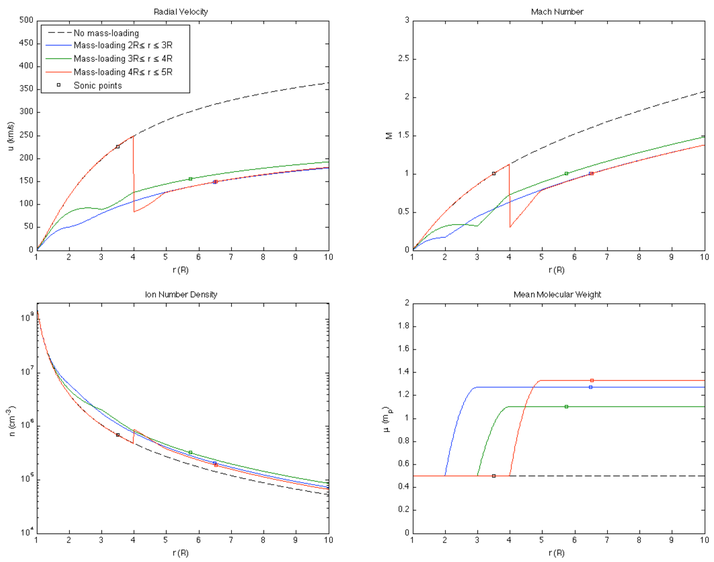

Figure 3: The solar wind being mass-loaded at various locations near the sun. The outermost sonic point is marked on each curve.

V. Results: Test Particle Transport

A test particle is added to the mass-loading solar wind, where radiation, gravitational, and Lorentz forces to act on it, along with ion drag from the wind (Draine and Salpeter, 1979). The test particle of radius a is chosen such that radiation and gravitational forces cancel out, leaving ion drag as the dominant force.

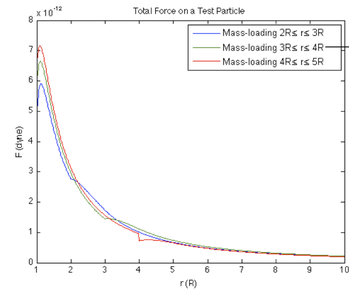

Figure 4: The total force on a test particle with radius $a = 0.23\mu m$ for each mass-loading case.

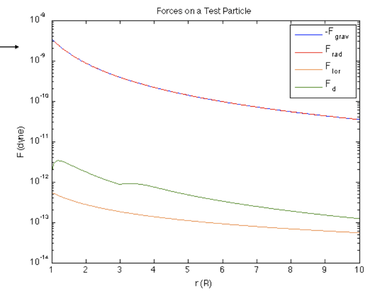

Figure 5: The individual forces on a test particle for a single mass-loading case.

For each case the path is calculated for a test particle of radius a. The test particle begins at rest at the leading edge of its respective mass-loading region.

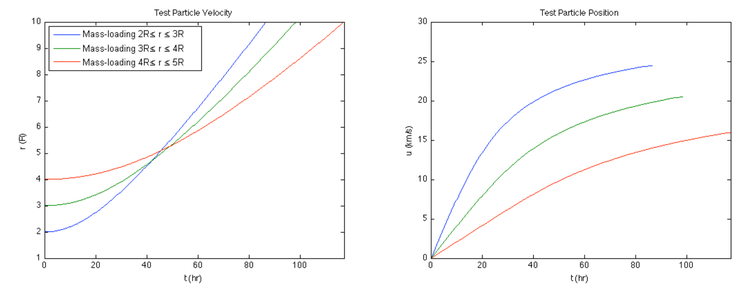

Figure 6: A test particle's position and velocity, calculated until reaching the outer boundary at $10R$.

VI. Future Work

These preliminary results give a general idea of how mass-loading due to dust is affecting the solar wind. To obtain more precise results, the next step forward would be to move from the simple 1D hydrodynamical model and study these mass-loading effects with a more advanced MHD model such as the Block-Adaptive-Tree-Solarwind-Roe-Upwind-Scheme (BATS-R-US) developed by the Center for Space Environment Modeling at the University of Michigan.

References

Biermann, L., B. Brosowski, and H. U. Schmidt: 1967, The interaction of the solar wind with a comet. *Solar Physics*, **1**, 254–284.

Draine, B. T. and E. E. Salpeter: 1979, On the physics of dust grains in hot gas. *Astrophysical Journal*, **231**, 77–94.

Gombosi, T. I., A. F. Nagy, and T. E. Cravens: 1986, Dust and neutral gas modeling of the inner atmospheres of comets. *Reviews of Geophyics*, **24**, 667–700.